

# Experimental characterization of the dynamic behavior of rolling tires

S. Vercammen, C. González Díaz, P. Kindt, J. Middelberg, C. Thiry, J. Leysens  
Goodyear Innovation Center Luxembourg, Tire Vehicle Mechanics Department  
Avenue Gordon Smith, L-7750, Colmar-Berg, Luxembourg  
e-mail: [stijn\\_vercammen@goodyear.com](mailto:stijn_vercammen@goodyear.com)

## Abstract

Although tire/road noise and tire vibration phenomena have been studied for decades, there are still some missing links in the process of accurately predicting and controlling the overall tire/road noise and vibration. An important missing link is represented by the effect of rolling on the dynamic behavior of a tire. Consequently, inside the European seventh framework program, an industry-academia partnership project, named TIRE-DYN, has been founded between KU Leuven, Goodyear and LMS International. By means of experimental and numerical analyses, the effects of rolling on the tire dynamic behavior are quantified.

This paper presents the results of vibration measurements on a rotating tire with an embedded accelerometer. Modal parameters of the rolling tire are estimated from an operational modal analysis. In addition, the dispersion curves, which give detailed insight in the wave propagation behavior of a structure, are analyzed for the rolling tire. The goal of these analyses is to deepen the understanding on the influence of rolling on the tire dynamic behavior.

## 1 Introduction

Noise resulting from road traffic has a severe impact on the environmental quality in urban areas all over the world. In the European Union, it is estimated that approximately 80 million people are exposed to unacceptably high noise levels [1]. The World Health Organization (WHO) and the Joint Research Centre of the Commission show that traffic-related noise may account for over 1 million healthy years of life lost annually in the EU member States and other Western European countries [2].

The noise generation from the interaction of rolling tires with the road surface is the most dominant source of vehicle noise for driving speeds above approximately 40 km/h for passenger cars. Although tire/road noise has been studied for several decades [3], there are still some missing links. One of the most important ones is the effect of rolling on the dynamic behavior of a tire [4]. Until now, several fragmented research efforts addressing the effects of rolling onto the tire dynamic properties have not yielded a full understanding of the complex dynamic behavior. This is mainly due to the strong multi-disciplinary character of the research subject. Therefore, inside the European seventh framework program, an industry-academia partnership project, named TIRE-DYN, has been founded between KU Leuven [5], Goodyear [6] and LMS International [7]. The project brings together academic and industrial knowledge and technology to quantify the effects of rolling on the tire dynamic behavior by means of experimental and numerical analyses. [8]

## 2 Basic concepts – analytical ring example

By means of an analytical ring example, this paragraph covers the basic theoretical concepts of the structural wave propagation in a tire.

When a tire is excited, structural waves propagate along the tire circumference. Bending, longitudinal and rotational waves can be identified. Propagating harmonic waves have the form of the following eqn. (1) [9]:

$$y = Ae^{j(kx-\omega t)} \quad (1)$$

with  $k$  the wave number and  $\omega$  the radial frequency of the wave. Equation (2) gives the relationship between the wavelength and the wave number, whereas eqn. (3) gives the relation between the time period and the frequency. These relations show that the wave number and radial frequency can be interpreted as the phase change of the wave per unit distance and time, respectively.

$$k = 2\pi/\lambda \quad (2)$$

$$\omega = 2\pi/T \quad (3)$$

Bolton et al. [10] characterized the wave propagation characteristics of a tire by means of a wave number decomposition of the radial tire vibrations. The dispersion relation expresses for each frequency, the wave numbers of the harmonic waves that can propagate in the structure. The graphical representation of the wave number decomposition is known as a dispersion graph. The dispersion graphs show the magnitude of the tire vibration velocity for each wave number/frequency combination due to a unit harmonic point force. Figure 1 shows an example of such a dispersion curve for an unloaded and non-rotating tire excited by a unit force at the tread center. The horizontal axis represents the real part of the wave numbers. Both positive and negative wave numbers are considered since waves propagate in both directions along the tire circumference. Each branch of the graph corresponds to a particular wave type. The bright spots correspond to tire resonances. At certain frequencies, waves travelling in opposite direction will interfere constructively and cause a standing wave pattern. The circumferential resonances appear when the tire circumferential length equals an integer multiple  $n$  of wavelengths. Equation (4) represents the condition for circumferential tire resonances, with  $R$  the tire radius and  $n$  an integer.

$$2\pi R = n\lambda \quad (4)$$

Substituting equation (2) into (4) yields the following condition for resonance:

$$k = n/R \quad (5)$$

The integer  $n$  is known as the circumferential mode number. It is the number of wavelengths in one tire circumference.

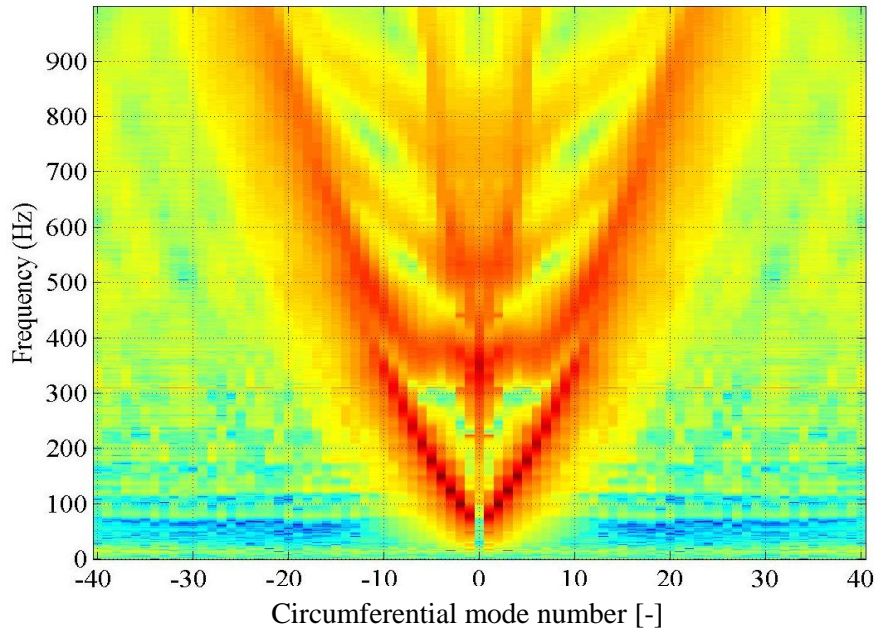


Figure 1: Example of dispersion curves for an unloaded and non-rotating tire, excited by a harmonic unit point force at the tread center

Figure 2 [11] provides more details on some of the wave types that propagate in an unloaded non-rotating tire.

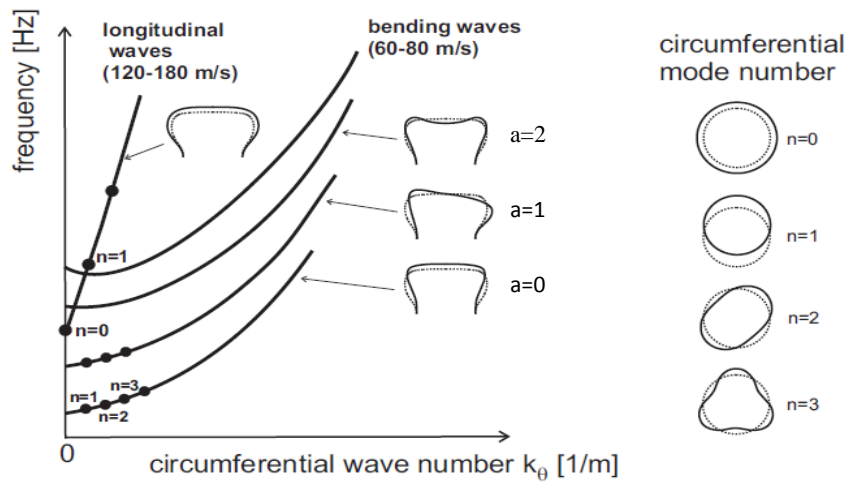


Figure 2: Typical dispersion curves corresponding different wave types for an unloaded and non-rotating tire

The tire resonance mode naming convention used in this research is based on the one introduced by Wheeler et al. [12] for modes of an unloaded tire. This convention uses two integer indices which describe the bending order of the belt package in two directions. The format of the notation is  $[n,a]$ . The first index  $n$  represents the number of circumferential bending wavelengths and is also known as the circumferential mode number. The second index  $a$  represents the number of half-wavelengths in the axial direction of the tread band at a circumferential location where the shape is at an extreme displacement. This convention is illustrated in figure 2. For a loaded and rotating tire, the naming convention needs to be extended to distinguish the different mode shapes. This is further discussed in the section on the experimental results.

In the lower frequency range, the dynamic behavior of a tire can be approximated by a flexible ring on an elastic foundation. The flexible ring represents the belt and tread layers; whereas, the elastic foundation represents the tire sidewalls. This simplified representation of the tire is used to analytically study the effects of rotation on the wave propagation in the tire. The most important conclusions from the analytical analysis are listed below and illustrated by figure 3 [4]:

1. A moving particle of the rotating ring is subjected to a **Coriolis acceleration**. This causes the circumferential phase speed of a forward and backward travelling wave to differ from each other.
2. For every circumferential mode number  $n$  larger than zero, the rotating ring has two resonances which appear at a different frequency. Moreover, the resonance frequencies are dependent on the rotational speed of the ring. This splitting of natural frequencies is known as the **bifurcation effect**. A dispersion curve in the co-rotating reference system becomes slightly asymmetric due to the rotation (figure 3(b)). Moreover, the speed of the flexural waves is increased due to the rotational stiffening (slope of the dispersion curve is increased). In the co-rotating reference frame, the mode shape associated with the highest resonance frequency  $\omega_{n1}$  is a **backward travelling wave** (travels in the opposite direction of the ring rotation). The mode shapes associated with the lowest resonance frequency  $\omega_{n2}$  is a **forward travelling wave**.
3. The travelling waves in the co-rotating reference system are observed in the fixed reference system as travelling waves at another frequency. This shift in the observed frequency is known as the Doppler shift and is illustrated in figure 3(c). The asymmetry of the dispersion curve due to the **Doppler shift** is much more pronounced than the asymmetry caused by the bifurcation effect.

For a non-rotating ring, a forward and backward travelling wave can interfere and form a standing wave pattern at the natural frequencies. In a rotating ring-like structure, a forward and backward travelling wave can no longer interfere at a single natural frequency to form a standing wave pattern due to the difference in propagation speed. At resonance, the rotating ring exhibits a travelling wave deformation pattern. To distinct the mode shapes exhibiting travelling wave behavior, the mode naming convention is extended with a plus sign for waves travelling in the tire rotational direction and minus sign for waves travelling against the tire rotation direction. Note that the flexible ring only approximates the dynamic behavior of a tire in unloaded condition.

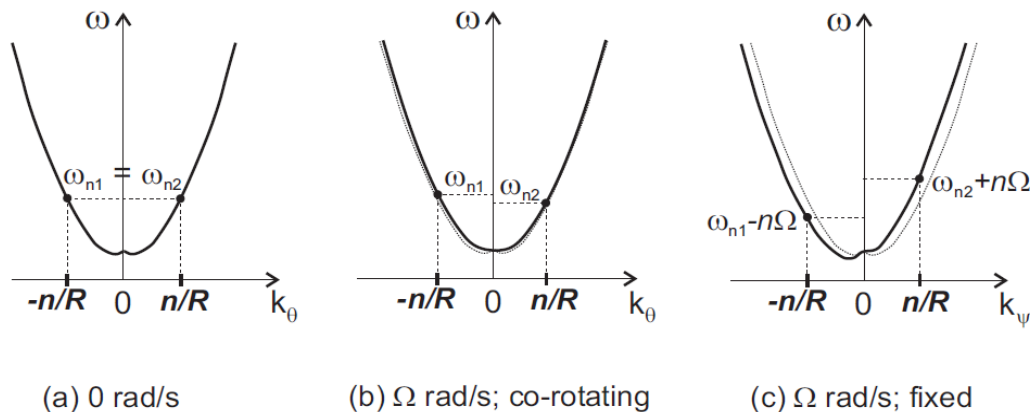


Figure 3: Dispersion curve of the: (a) non-rotating ring; (b) rotating ring in a co-rotating axis system; (c) rotating ring in a fixed axis system. The dots on the dispersion curve represent a mode with a circumferential mode number  $n$  ( $n = 1, 2, 3, \dots$ ) (shape of the curves based on [13])

### 3 Experimental analysis – Accelerometer measurements

This section describes the experimental characterization of the dynamic behavior of a tire in loaded and rolling conditions by means of accelerometer measurements. The measurements, post-processing of the data and the final results are discussed.

The tire is rolling on a steel drum and excited by a metal strip attached to the drum, called a cleat. The tire structural response is obtained from an accelerometer mounted at the center of the inner liner of the tire. The accelerometer is uniaxial, therefore only radial vibrations are measured. The measurement conditions are listed in table 1.

Measurement conditions	
Tire dimensions	205/55 R16
Inflation pressure [bar]	2.2
Load [N]	4000
Cleat dimensions [mm]	3x25
Steel drum diameter [m]	2
Speeds [km/h]	40, 60 & 80
Sampling frequency [kHz]	32

Table 1: The experiments were performed under the following measurement conditions

In case the drum radius is not an exact multiple of the effective tire radius, which is practically always the case, the accelerometer position with respect to the cleat impact shifts for every drum rotation. During one drum rotation the number of tire rotations depends on the ratio between the effective tire and drum radius. To determine the phase relation between the accelerometer and cleat, for every single measurement point, also tire tacho and drum tacho signals are recorded.

The measured radial tire vibration data in the co-rotating axis system is converted into the fixed axis system to yield the acceleration responses to the cleat impact in 360 distinct fixed points, equally spaced around the circumference of the tire. The resulting spatial resolution of  $1^\circ$  is largely sufficient for the wave number range investigated in this paper. The obtained frequency resolution on the other hand, equals the inverse of the acceleration response signal time length. This is limited by the time for one drum revolution. Therefore, the smallest frequency resolutions will be achieved at the lowest speed.

As an example, figure 4 shows the first 0.2 s (of 0.37 s) of an acceleration response signal at the tire leading edge at 45 degrees from the footprint contact. The tire is rolling at 60 km/h over a 25 mm long cleat with a height of 3 mm.

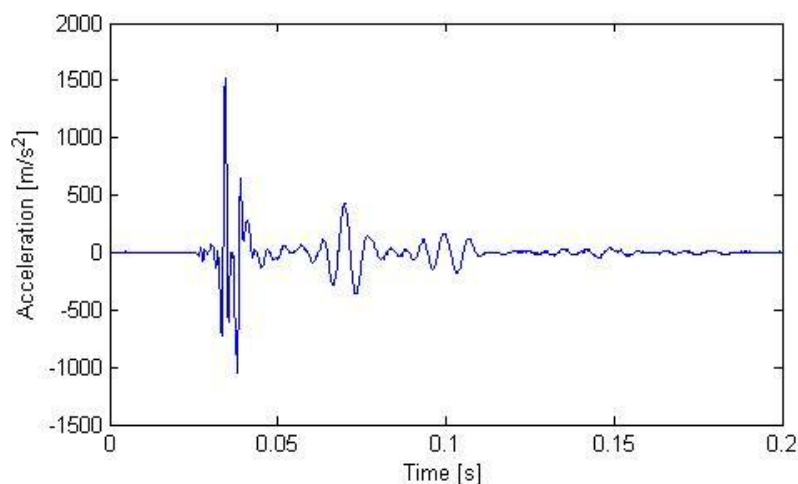


Figure 4: Acceleration response signal at the leading edge at 45 degrees from the footprint contact (cleat 3x25 mm, 60 km/h)

The transformation of acceleration responses from time to frequency and space to wave number domain respectively, yields the dispersion graph of the tire at the specified measurement conditions. Figure 5 shows the dispersion graphs for speeds 40, 60 and 80 km/h. As discussed in the introduction, the dispersion graph contains information on the wave propagation properties which determine the tire dynamic behavior.

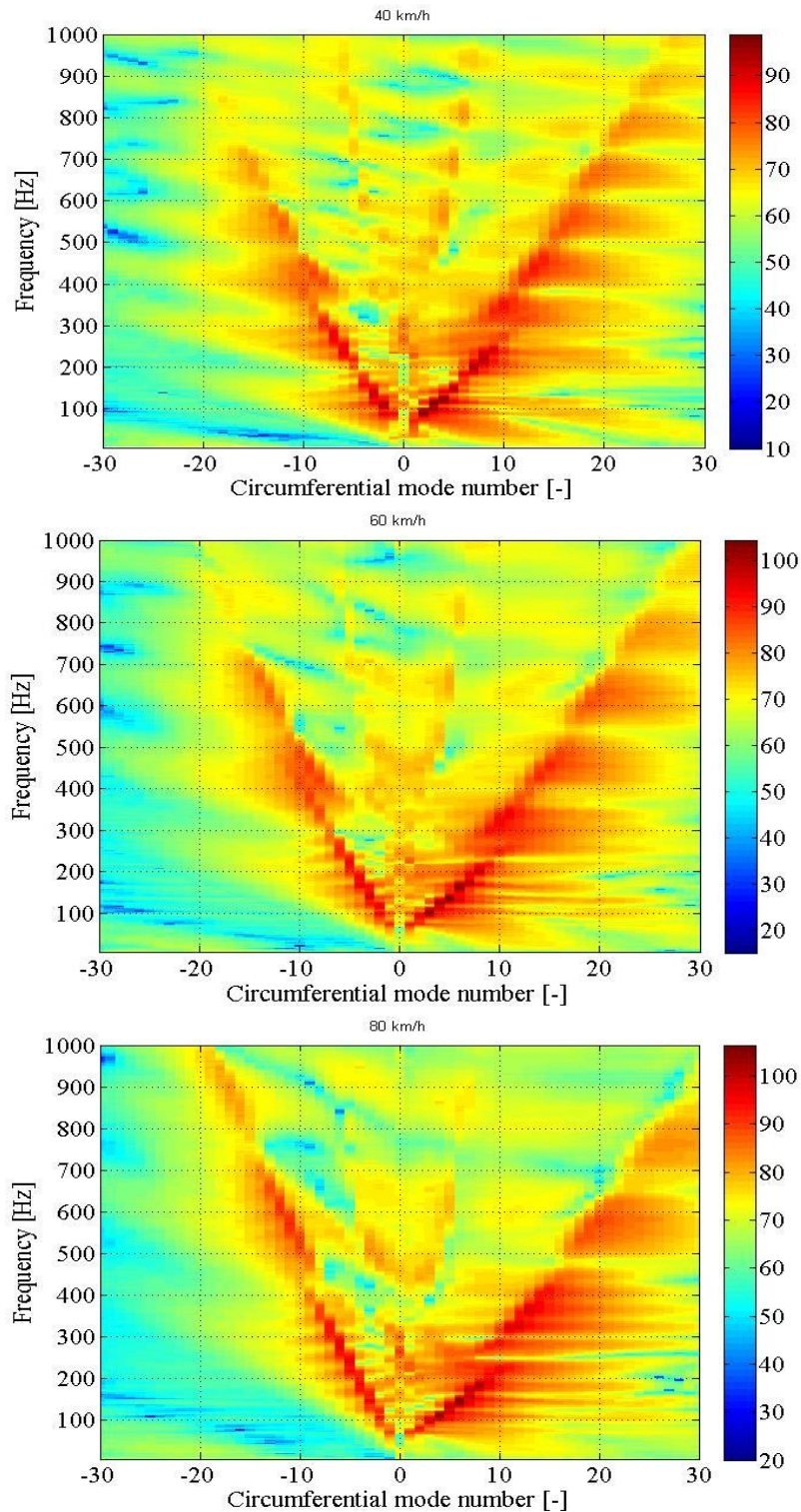


Figure 5: Dispersion graphs for speeds 40, 60 & 80 km/h. The positive circumferential mode numbers correspond to waves travelling opposite to the tire rotational direction and negative wave numbers to waves travelling in the tire rotational direction

In order to estimate the modal parameters of the rolling tire, the polyreference least squares complex exponential method [14] is applied to auto- and cross-correlation functions between the acceleration signals and one or more selected reference signals. Since the input signal (cleat impact) is unknown, no classical modal analysis methods on the basis of frequency response functions can be applied to estimate the modal parameters. Therefore, an operational modal analysis is performed, which is based on output signals only. The correlation functions between two response signals can be decomposed as a sum of decaying sinusoids where each sinusoid has a damped natural frequency and damping ratio. This decomposition of sinusoids and matching mode shapes, fully characterizes the tire's dynamic behavior.

Figure 6 shows the identified mode shapes for the reference case. The grey arrow indicates the tire rotational direction while the red arrow indicates the direction of the travelling wave. The blue dots indicate nodal points (points which for a certain mode shape exhibit no deformation). Standing wave modes can be observed for low wave numbers (and low speeds) where the wave propagation properties of the positive and negative going wave do not deviate too much. In that case the waves traveling in opposite direction could still interfere constructively and form a standing wave pattern.

On the measured dispersion curves it can be observed that the waves travelling opposite to the tire rotational direction have higher response amplitudes with respect to the waves traveling in the rotational direction. Therefore, mainly modes corresponding to traveling waves in the direction opposite to the rotation are identified from the operational modal analysis.

Note that the circumferential mode number, which equals the number of circumferential bending wavelengths, is no longer necessarily an integer, as opposed to the non-rotating case. This is due to the footprint which acts as a boundary condition to the travelling waves.

The excitation strongly determines the possibility to identify certain modes. Figure 7 shows simulated vertical and fore-aft input forces of the cleat impact in the frequency domain. The force distribution is not uniform. This is also reflected in the dispersion graphs of figure 5 with higher and lower amplitude regions. Modes that are not well excited are less likely to be identified. The same accounts for the higher order branches:  $[n,1]$ ,  $[n,2]$ , ... which are less well excited compared to the  $[n,0]$  branches since the cleat excites the tire over its whole width.

For higher wave numbers and corresponding frequencies it becomes harder to identify distinct modes. This is caused by the combination of a high modal density, the tire damping and the fact that the waves with higher wave numbers are less well excited (see figure 7). Due to the above mentioned reasons, above a certain wave number the modal parameter estimation algorithm is not anymore able to distinguish different modes.

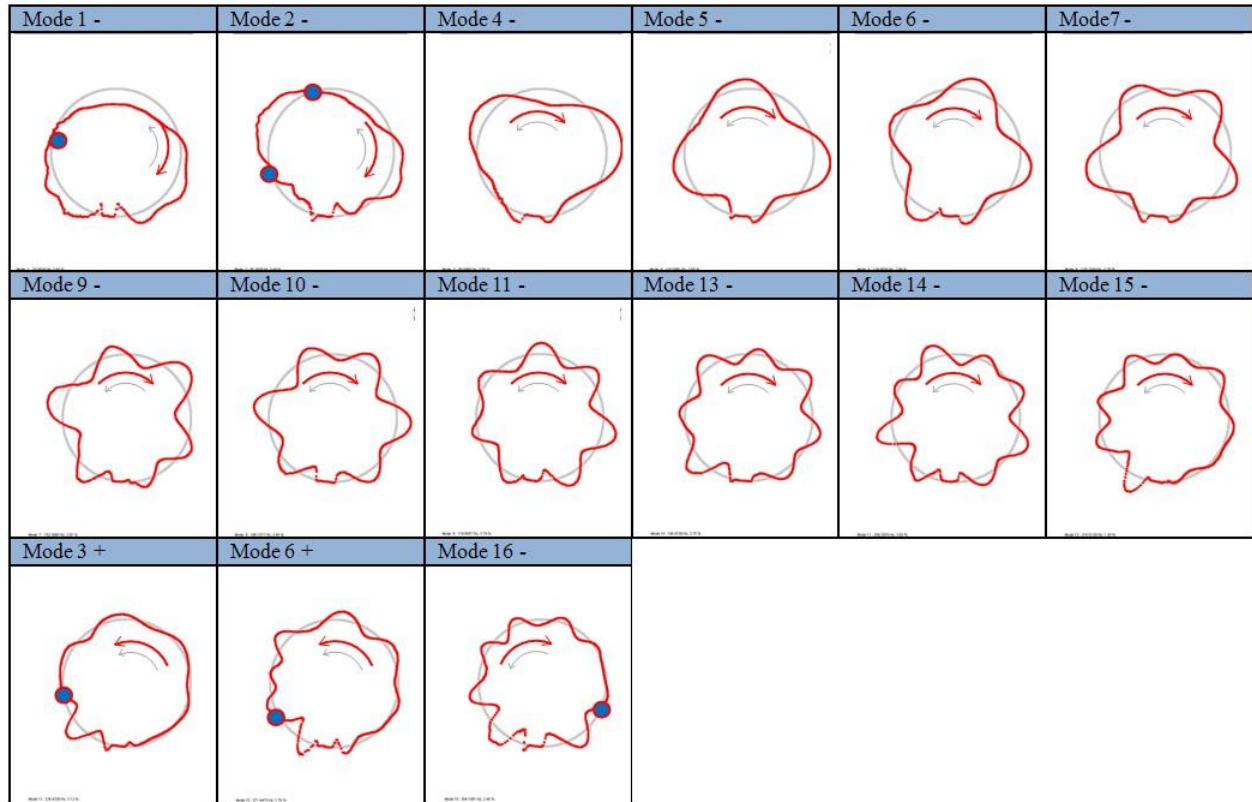


Figure 6: Identified mode shapes of tire at the following conditions: 60 km/h, cleat 3x25 mm, 4000 N, 2.2 bar

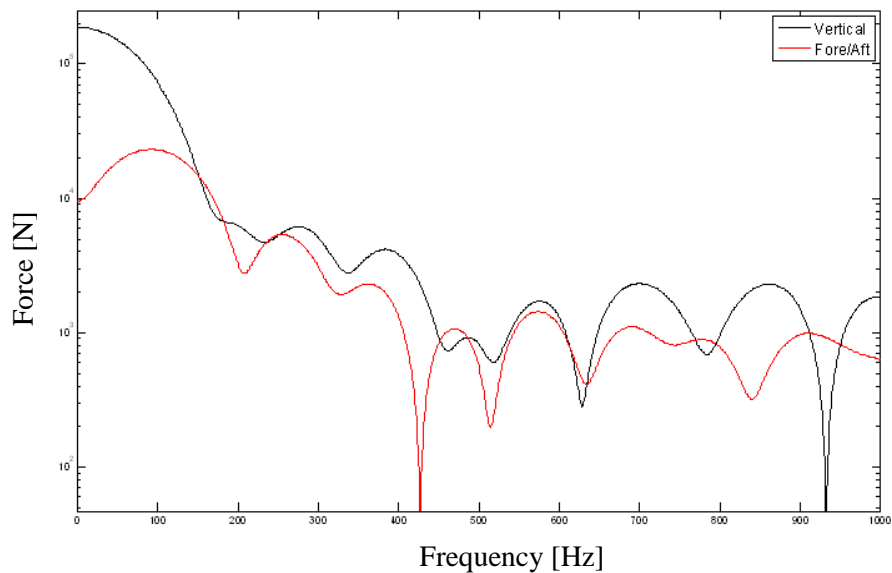


Figure 7: Simulated spectra of the vertical and fore-aft input forces for the considered tire rolling at 60 km/h over a 3x25 mm cleat

Table 2 and table 3 show the natural frequencies and modal damping of the identified modes for speeds 40, 60 and 80 km/h. They correspond to the lower two branches of the dispersion graphs (figure 5). Since the analysis is performed in a fixed axis system, resonance frequencies are subjected to the Doppler shift as discussed for the flexible ring analytical example. By deducting the Doppler shift, the natural

frequencies observed in the co-rotating axis system can be calculated. Figure 8 shows a graphical presentation of this data. This graph clearly shows that the resonance frequencies shift depending on the tire rotational speed.

Mode	40 km/h		60 km/h		80 km/h	
	$f_{nat}$ [Hz]	$\xi$ [%]	$f_{nat}$ [Hz]	$\xi$ [%]	$f_{nat}$ [Hz]	$\xi$ [%]
Mode 1 -	71.74	7.96%	73.48	4.98%	72.51	4.49%
Mode 2 -	90.19	4.72%	87.43	3.75%	84.24	4.86%
Mode 3 -	101.49	3.45%				
Mode 4 -	115.26	3.26%	99.34	3.96%	96.53	4.14%
Mode 5 -	127.71	3.15%	111.70	3.42%	107.72	3.22%
Mode 6 -	143.07	2.70%	124.85	3.48%	119.23	3.21%
Mode 7 -	155.19	2.56%	138.21	3.28%		
Mode 8 -					133.47	2.92%
Mode 9 -	165.47	2.14%	152.37	2.92%	146.72	3.18%
Mode 10 -			166.15	3.45%		
Mode 11 -	185.62	2.75%	179.81	3.79%	158.04	4.41%
Mode 12 -	202.41	3.37%			176.25	3.23%
Mode 13 -	216.71	2.36%	195.47	3.75%	186.80	3.38%
Mode 14 -	234.02	2.07%	209.29	3.78%		
Mode 15 -	251.02	2.35%	218.51	1.28%		

Table 2: Natural frequencies ( $f_{nat}$ ) and modal damping ( $\xi$ ) of the identified “-“ modes for speeds 40, 60 & 80 km/h

Mode	40 km/h		60 km/h		80 km/h	
	$f_{nat}$ [Hz]	$\xi$ [%]	$f_{nat}$ [Hz]	$\xi$ [%]	$f_{nat}$ [Hz]	$\xi$ [%]
Mode 1 +	77.78	6.59%				
Mode 2 +					214.81	2.58%
Mode 3 +			236.38	3.14%	240.86	1.80%
Mode 4 +					261.11	3.12%
Mode 5 +	251.02	2.35%			277.52	2.67%
Mode 6 +			271.56	1.82%	289.65	2.78%
Mode 7 +	280.35	2.59%				
Mode 8 +	310.70	2.24%				

Table 3: Natural frequencies ( $f_{nat}$ ) and modal damping ( $\xi$ ) of the identified “+“ modes for speeds 40, 60 & 80 km/h

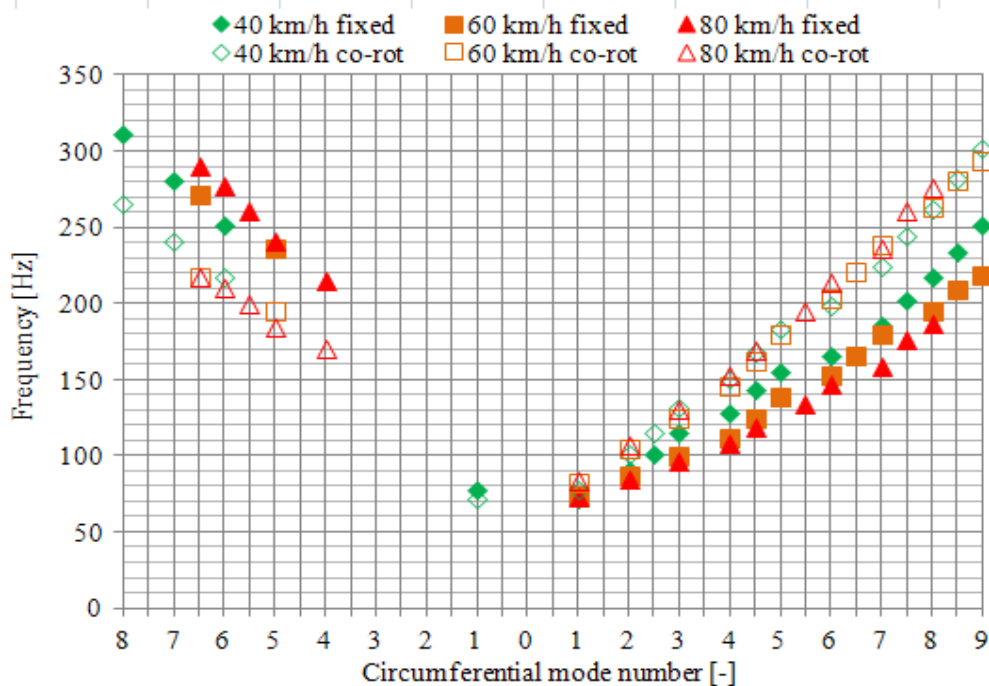


Figure 8: Graphical representation of the natural frequencies of the identified modes for speeds 40, 60 & 80 km/h, in a fixed and co-rotating axis system

## 4 Conclusions

This paper analyses the effects of rotation on the dynamic behavior of a loaded and rotating tire. The analysis is based on experiments where an accelerometer is attached to the inner liner of a tire.

The results show the dependency of the tire dynamic behavior with respect to the rotational speed. The rotating tire is subjected to Coriolis accelerations which makes the wave speed of the waves travelling in opposite direction of the tire rotation to diverge from the speed of the waves travelling in the rotation direction. This leads to complex or travelling mode shapes. While for a non-rotating tire the mode shapes are real or standing waves. The results also show how the footprint contact, established due to loading of the tire, acts as a boundary condition for the structural waves and thus influences the dynamic behavior of the rolling tire.

## 5 Acknowledgments

The research reported has been performed in the framework of the FP7 Marie Curie IAPP project “TIRE-DYN” (FP7-PEOPLE-IAPP2009, Grant Agreement No. 251211).

## 6 References

- [1] Coordination of European Research for Advanced Transport Noise Mitigation (CALM), *Research for a quieter Europe in 2020: Updated strategy paper of the CALM II network*, (2007).
- [2] World Health Organization (WHO) and Joint Research Centre of the Commission, *Report on Burden of disease from environmental noise*, [www.euro.who.int/en/what-we-do/health-topics/environmental-health/noise](http://www.euro.who.int/en/what-we-do/health-topics/environmental-health/noise), (2011).

- [3] U. Sandberg, J.A. Ejsmont, *Tyre/road Noise Reference Book*, Informex Ejsmont & Sandberg Handelsbolag, Harg, SE-59040, Sweden, Kisa (2002).
- [4] P. Kindt, *PhD thesis on Structure-Borne Tyre/Road Noise due to Road Surface Discontinuities*, ISBN 978-94-6018-085-9, Leuven (2009).
- [5] Katholieke Universiteit Leuven, Department of mechanical engineering, Leuven, Belgium, [www.mech.kuleuven.be](http://www.mech.kuleuven.be)
- [6] Goodyear Innovation Center, Colmar-Berg, Luxembourg, [www.goodyear.com](http://www.goodyear.com)
- [7] LMS International, HQ and Engineering Innovation Center, Leuven, Belgium, [www.lmsintl.com](http://www.lmsintl.com)
- [8] EU FP7 IAPP TIRE-DYN, Grant Agreement 251211, *Experimental and Numerical Analyses of the Dynamic Behavior of Rolling Tires in order to Improve the Tire Modeling Accuracy*, [www.tiredyn.org](http://www.tiredyn.org)
- [9] K.F. Graff, *Wave motion in elastic solids*, Oxford University Press, (1975).
- [10] J.S. Bolton, Y.J. Kim, *Wave Number Domain Representation of Tire Vibration*, Internoise 2000, France, Nice (2000).
- [11] J.S. Bolton, Y.J. Kim, *Technical report on Visualization of the tire vibration and sound radiation and modeling of tire vibration with an emphasis on wave propagation*, The Institute for Safe, Quiet and Durable Highways, <http://ntl.bts.gov/lib/24000/24600/24635/index.html>, (2003)
- [12] R.L. Wheeler, H.R. Dorfi, B.B. Keum, *Vibration modes of radial tires: measurement, prediction, and categorization under different boundary and operating conditions*, (2005).
- [13] Y.J. Kim, J.S. Bolton, *Effects of rotation on the dynamics of a circular cylindrical shell with application to tire vibration*, *Journal of Sound and Vibration*, 275:605-621, (2004)
- [14] L. Hermans, H. Van der Auweraer, *Modal testing and analysis of structures under operational conditions: Industrial applications*, *Mechanical Systems and Signal Processing*, 13(2):193–216, (1999).

